

## Solid Nitrogen: A Nuclear Quadrupole Resonance Study\*

J. R. Brookeman, M. M. McEnnan, and T. A. Scott

*Department of Physics, University of Florida, Gainesville, Florida 32601*

(Received 7 June 1971)

Nuclear quadrupole resonance of  $^{14}\text{N}$  ( $I=1$ ) has been studied for the two diatomic species  $^{14}\text{N}-^{14}\text{N}$  and  $^{14}\text{N}-^{15}\text{N}$  in solid  $\alpha$ -nitrogen. Spectra from carefully prepared and annealed samples display well-resolved intramolecular dipolar splittings consisting of an asymmetric triplet for  $^{14}\text{N}-^{14}\text{N}$  and a doublet for  $^{14}\text{N}-^{15}\text{N}$ . From the order of the components of the triplet, the sign of the nuclear quadrupole coupling constant is deduced to be negative. Measurements of the resonance frequencies  $\nu_Q(14-14)$  and  $\nu_Q(14-15)$  have been made as a function of temperature from 4.2 K to the phase transformation at 35.6 K, and as a function of isotopic concentration for five concentrations ranging from 0.37 to 99%  $^{15}\text{N}$ . The hydrostatic pressure dependence of  $\nu_Q(14-14)$  in a natural isotopic abundance sample has been observed at seven fixed temperatures. These results were combined with detailed thermal expansion and compressibility data to obtain the resonance frequency  $\nu_Q(14-14)$  as a function of temperature at constant volume and as a function of volume at constant temperature. The observed strong temperature dependence of the resonance frequency is ascribed to excitation of large-amplitude molecular librations having substantial anharmonic character. A quasiharmonic theory of motional averaging incorporating published Raman spectroscopy data provides a satisfactory fit to the resonance frequency at zero pressure. An independent determination of the motional averaging obtained from the dipolar splitting is in excellent agreement with the averaging of the quadrupole resonance frequency. A fit of the theoretical equation for motional averaging with the experimental volume dependence of  $\nu_Q(14-14)$  yields the volume dependence of the libration frequencies. Three isotopic mass effects were observed and studied at 4.2 K: (i) The frequencies  $\nu_Q(14-14)$  and  $\nu_Q(14-15)$  increase approximately linearly with increasing concentration of  $^{15}\text{N}$  (isotope shift); (ii)  $\nu_Q(14-15) - \nu_Q(14-14) = 7.95 \pm 0.30$  kHz independent of concentration (isotope splitting); and (iii) the individual lines of the spectra broaden in mixed samples due to dynamic disorder. The total isotope shift is  $2.6 \pm 0.25$  kHz for both molecules; a qualitative explanation of the effect is given based on the volume dependence of  $\nu_Q(14-14)$ , the known difference in lattice constants of pure  $^{14}\text{N}_2$  and  $^{15}\text{N}_2$ , and the assumption of a defect volume for a  $^{14}\text{N}-^{14}\text{N}$  impurity molecule in a  $^{15}\text{N}_2$  lattice. The isotope splitting is a consequence of unequal masses and force constants for the two molecules.

### I. INTRODUCTION

Nitrogen is known to crystallize in three structures<sup>1-3</sup> ( $\alpha$ ,  $\beta$ , and  $\gamma$ ) depending on the pressure and temperature. The  $\alpha$  and  $\beta$  phases occur at equilibrium vapor pressure whereas the  $\gamma$  phase exists only at applied pressures<sup>4</sup> greater than about 3500 atm. This paper is concerned exclusively with a nuclear quadrupole resonance (NQR) study of the  $\alpha$  phase, which at equilibrium vapor pressure is stable below 35.6 K. The crystal structure of  $\alpha$ -nitrogen is primitive cubic with a basis of four molecules per unit cell. The molecules are orientationally ordered in the basis such that a molecule is aligned parallel to each of the four body diagonals of the cube. Assignment of the space group to either  $P2_13$  or  $Pa3$  has not been completely settled in the literature. The most recent x-ray analysis<sup>1</sup> favors  $P2_13$ , but Raman<sup>5-7</sup> and infrared spectroscopy<sup>8,9</sup> and electron diffraction<sup>10</sup> work find no evidence of this structure and are consistent with  $Pa3$ . The molecules lie on a center of symmetry in the  $Pa3$  structure, whereas in  $P2_13$  each molecular center is displaced along a cube body diagonal. In

fact, there is a simple test between the two structures that seems not to have been tried. The non-centrosymmetric  $P2_13$  space group must be piezoelectric. A frequency-modulated nuclear resonance spectrometer, such as used in this work, happens to be a sensitive detector of piezoelectric resonances and we find weak piezoelectric resonances by this method in  $\alpha$ -nitrogen.<sup>11</sup> There is, therefore, no doubt that the correct assignment is  $P2_13$ .

Orientalional ordering and lattice dynamics in  $\alpha$ -nitrogen have been discussed in numerous papers.<sup>12-16</sup> Various forms of the intermolecular potential have been examined: (i) the superposition of a spherically symmetric Lennard-Jones potential with an anisotropic part due to either (a) molecular quadrupole quadrupole (MQQ) interactions or (b) MQQ interactions plus directional corrections to the attractive dispersive and repulsive forces, and (ii) an atom-atom Lennard-Jones potential. None of these potentials has been entirely successful in explaining all the features of the solid, but all predict the molecular ordering provided by either the  $Pa3$  or  $P2_13$  crystal structure. The ori-

entational potential is of paramount importance in determining many of the physical properties of  $\alpha$ -nitrogen. Because the potential is weak, large-amplitude librations of the molecules occur about the equilibrium positions and contribute to strong temperature dependences of thermal expansion,<sup>17</sup> compressibility,<sup>17</sup> specific heat,<sup>18,19</sup> and, as we shall emphasize here, the NQR spectra. A striking demonstration that the stability of the  $\alpha$  phase is dependent upon the anisotropic part of the intermolecular potential is provided by experiments in which argon atoms are substituted in the lattice.<sup>20</sup> The stability range of  $\alpha$ -nitrogen decreases rapidly with increasing concentration of the spherically symmetric argon atoms and disappears entirely at less than 25% argon.

A number of other important low-temperature solids crystallize in the  $Pa3$  or  $P2_13$  structures. Among these are orthohydrogen, paradeuterium, carbon monoxide, carbon dioxide, nitrous oxide, and ammonia. Thus, a thorough study of nitrogen has ramifications extending beyond the material itself.

Several physical properties of nitrogen are almost ideally convenient for study by means of NQR; indeed, it is exceptional to find such a fortunate confluence of subject and method. Because the molecular bond is vastly stronger than the solid-state bond, the molecule remains a well-defined entity in the solid and the electric field gradient at the nuclear site is almost entirely of intramolecular origin; over-all cubic symmetry also leads to a reduction of the intermolecular contribution to the electric field gradient. Furthermore, the intramolecular nuclear separation is 1.10 Å, whereas the closest distance between nuclei on neighboring molecules is 3.42 Å. Therefore, the magnetic dipole pairs within a molecule interact strongly but are relatively isolated from other molecules. Thus, one deals with a simple quasi-isolated two-spin system and the NQR spectrum basically provides information about the static and dynamic properties of individual molecules in the solid. Two stable isotopes occur,  $^{14}\text{N}$  ( $I=1$ ) and  $^{15}\text{N}$  ( $I=\frac{1}{2}$ ). The natural abundance is 99.63%  $^{14}\text{N}$ , but samples enriched in  $^{15}\text{N}$  are readily obtainable. Thus, NQR of  $^{14}\text{N}$  can be observed in two of three possible diatomic species, viz.,  $^{14}\text{N}-^{14}\text{N}$  and  $^{14}\text{N}-^{15}\text{N}$ .

Experimental data on the temperature dependence of the NQR frequency and relaxation time in  $\alpha$ -nitrogen have been presented in previous papers<sup>21-23</sup> and discussed in terms of simplified models for the lattice dynamics. Extensive new experimental work on nitrogen that has been conducted recently in our laboratory<sup>17,24-27</sup> and elsewhere permits a thorough analysis of the solid without many of the approximations that must normally be made in interpreting NQR data. The normal-mode problem for the op-

tical frequencies has been solved and the degeneracies of the vibrations are known.<sup>28</sup> The libration frequencies, which play a dominant role in the temperature dependence of the NQR as well as the thermal stability of the solid, have all been measured by Raman spectroscopy<sup>5-7</sup> at several temperatures. The compressibility and thermal expansion<sup>17</sup> have been measured between 4.2 K and the phase transition, and the compressibility is also known as a function of pressure.<sup>29</sup> Finally, we have obtained the pressure dependence of the resonance frequency for a number of temperatures and have studied three second-order isotope effects due to the different mass and nuclear spin of  $^{14}\text{N}$  and  $^{15}\text{N}$ . So much detailed and related information has never been available for interpretation of NQR data in any material. As we shall demonstrate in this and a subsequent paper, the NQR data provide an exceedingly sensitive probe of molecular dynamics of solid nitrogen.

## II. EXPERIMENTAL

Research-grade nitrogen (99.999% pure) obtained from Air Products and Chemicals Inc. was used for the experiments on natural-abundance samples. Isotopically enriched gas was purchased from Isomet Corporation. Success in the line-shape studies was critically dependent on sample preparation. Liquid nitrogen was condensed into a 1.5-cm<sup>3</sup> glass sample chamber inside the rf coil. This sample was solidified slowly to form a single crystal of  $\beta$ -nitrogen and then cooled slowly to the phase transition temperature  $T_{\alpha\beta}$  at 35.6 K. Over a period of hours the sample was taken through the crystallographic transformation and then annealed many hours more (~10 h) at a temperature approximately 0.1 K below  $T_{\alpha\beta}$ . It is possible that a single crystal was produced by this procedure, but this was not checked since the fact is inconsequential for the data analysis.

The annealing procedure and also the strong temperature dependence of the quadrupole resonance frequency above 25 K required sensitive temperature regulation. A precision temperature-control cryostat similar to one described previously,<sup>30</sup> but of improved design, was used. Temperature measurements were made with a platinum resistance thermometer calibrated by the National Bureau of Standards and a germanium resistance thermometer. Automatic temperature regulation based on the germanium thermometer was achieved using a Leeds and Northrup model No. 7556-A potentiometer with the null-detector unbalance feeding a programmable power supply that controlled a heater on a copper shield surrounding the sample chamber. This system provided a uniform temperature over the sample with a resolution and long-term stability of a few millidegrees.

For the pressure studies, 7 cm<sup>3</sup> of nitrogen was condensed into a beryllium-copper (Be-Cu) pressure bomb of conventional design.<sup>31</sup> Sealing of the bomb was accomplished with an annealed Be-Cu ring for the plug and a pipestone cone for the rf feed-through. The nitrogen sample was pressurized with helium gas and the pressure was measured with a calibrated Bourdon gauge accurate to 0.1%. Pressure was generated with a two-stage system consisting of a 2-kbar gas booster pump in series with a 7-kbar intensifier. Data were taken only when the system was perfectly leak-tight. An x-ray diffraction study of solid nitrogen pressurized with helium gas has shown no evidence of penetration of the helium into the nitrogen lattice.<sup>3</sup> Our NQR results likewise show no effects of lattice distortion even though on one occasion high pressure was applied almost continuously over a period of a week. The NQR line shapes, which would be very sensitive to nonuniform stress, indicate that the pressure on the solid was at all times hydrostatic to at least one part in a thousand.

The resonance lines were detected with a conventional Robinson oscillator.<sup>32</sup> Small-amplitude frequency modulation with lock-in amplifier detection provided a derivative recording of the line shapes with negligible distortion. Helmholtz coils were used to cancel the earth's magnetic field at the sample. For the weak signals encountered in the isotope concentration study, many scans through the resonance were accumulated from the output of the lock-in amplifier and stored in a Fabritek 1070 digital signal averager. For the lowest concentrations of the isotope study the weak NQR signal was normally superimposed on comparably weak piezoelectric resonances resulting from the noncentrosymmetric *P*<sub>213</sub> crystal structure of  $\alpha$ -nitrogen. This problem was readily circumvented as follows: After accumulating a number of normal scans, a strong inhomogeneous magnetic field was applied to the sample to wipe out the NQR signals and the scan was repeated. The piezoelectric signals are unaffected by the magnetic field and by storing these results in separate sections of the Fabritek memory and then subtracting, the NQR spectrum could be extracted.

### III. HAMILTONIANS AND SPECTRAL ANALYSIS

#### A. Theory

##### 1. Intramolecular Interactions

For the reasons given in the Introduction, the NQR spectra of  $\alpha$ -nitrogen are dominated by intramolecular interactions. The quadrupole Hamiltonian for a single nucleus of spin  $I = 1$  and nuclear quadrupole moment  $eQ$ , subjected to an axially symmetric electric field gradient  $eq$ , is given by

$$\mathcal{H}_Q = \frac{1}{4} e^2 q Q (3I_z^2 - \bar{I}^2). \quad (1)$$

Splittings within the NQR spectra are produced through perturbation of the quadrupole interaction  $\mathcal{H}_Q$  of the resonant <sup>14</sup>N nuclei, by the intramolecular magnetic dipole-dipole interaction  $\mathcal{H}_d$ , and the indirect spin-spin interaction  $\mathcal{H}_J$ . These Hamiltonians expressed in the principal axes system of the electric field gradient (EFG) tensor for the axially symmetric N<sub>2</sub> molecule are

$$\mathcal{H}_d = h^2 \gamma_1 \gamma_2 r_{12}^{-3} \left[ \frac{1}{2} (I_{1+} I_{2-} + I_{1-} I_{2+}) - 2 I_{1Z} I_{2Z} \right], \quad (2)$$

$$\mathcal{H}_J = h \left[ \frac{1}{2} J_{\perp} (I_{1+} I_{2-} + I_{1-} I_{2+}) + J_{\parallel} I_{1Z} I_{2Z} \right], \quad (3)$$

where  $Z$  is along the molecular axis,  $r_{12}$  is the distance between nuclei within a molecule, and  $J_{\perp}$  and  $J_{\parallel}$  are components of the indirect spin-spin interaction. The other symbols have their conventional meanings. For the two molecular species <sup>14</sup>N-<sup>14</sup>N and <sup>14</sup>N-<sup>15</sup>N, respectively, the full Hamiltonians may be written in symbolic form as

$$\begin{aligned} \mathcal{H}(14-14) = & \mathcal{H}_{Q1}(14-14) + \mathcal{H}_{Q2}(14-14) + \mathcal{H}_d(14-14) \\ & + \mathcal{H}_J(14-14), \quad (4) \end{aligned}$$

$$\mathcal{H}(14-15) = \mathcal{H}_{Q1}(14-15) + \mathcal{H}_d(14-15) + \mathcal{H}_J(14-15). \quad (5)$$

For the *P*<sub>213</sub> structure the possibility exists that  $\mathcal{H}_{Q1} \neq \mathcal{H}_{Q2}$  because opposite ends of a molecule have somewhat different nearest-neighbor configurations. However, no definite experimental evidence has been found for a difference and the two terms are evidently equal to within a few parts in 10<sup>5</sup>. This fact is only one of several indications for the dominance of the intramolecular EFG. Because of dynamic effects,  $\mathcal{H}_Q(14-15) \neq \mathcal{H}_Q(14-14)$ . This isotope effect will be discussed in Sec. V.

Because  $\mathcal{H}_Q$  is some three orders of magnitude larger than  $\mathcal{H}_d$  and  $\mathcal{H}_J$ , first-order perturbation theory is sufficient to obtain the level shifts due to  $\mathcal{H}_d$  and  $\mathcal{H}_J$ . The allowed transition frequencies and relative intensities for the two molecules are listed in Table I for the case in which the quadrupole coupling constant  $A = e^2 q Q / 4h$  is negative. Changing the sign of the coupling constant reverses the splittings in each spectrum about the unperturbed frequency  $\nu_Q = 3|A|$ . Inasmuch as the <sup>14</sup>N-<sup>14</sup>N spectrum is asymmetric, the correct sign may be deduced from observation. The dipolar coupling constants  $d_{12} = h\gamma_1\gamma_2/2\pi r_{12}^3$  and the spin-spin coupling constants of the two molecular species are related by

$$d(14-15) = (\gamma_{15}/\gamma_{14})d(14-14),$$

$$J(14-15) = (\gamma_{15}/\gamma_{14})J(14-14),$$

where the magnetogyric ratios have the values  $\gamma_{14}/2\pi = 3.076 \times 10^2$  Hz/G and  $\gamma_{15}/2\pi = -4.315 \times 10^2$  Hz/G.

TABLE I.  $^{14}\text{N}$  NQR transition frequencies and relative intensities for  $^{14}\text{N}$ - $^{14}\text{N}$  and  $^{14}\text{N}$ - $^{15}\text{N}$  molecules. Intramolecular magnetic dipole-dipole and indirect spin-spin interactions are treated as perturbations to first order in the parameters  $d_{12} = \gamma_1\gamma_2\hbar/2\pi r_{12}^3$ ,  $J_{\parallel}$ , and  $J_{\perp}$ . Parameters for the two molecules are related by  $d(14-14) = d(14-15) \times (\gamma_{14}/\gamma_{15}) \equiv d$  and  $J(14-14) = J(14-15)(\gamma_{14}/\gamma_{15}) \equiv J$ . The quadrupole coupling constant  $A = e^2qQ/4\hbar$  is negative.

Molecule	Transition frequency	Relative intensity
$^{14}\text{N}$ - $^{14}\text{N}$	$3  A(14-14)  + 3d + J_{\perp} - J_{\parallel}$	2
	$3  A(14-14)  - d + J_{\perp} + J_{\parallel}$	1
	$3  A(14-14)  - d - J_{\perp}$	2
	$3  A(14-14)  - 3d - J_{\perp} + J_{\parallel}$	1
$^{14}\text{N}$ - $^{15}\text{N}$	$3  A(14-15)  + \frac{1}{2}(2d - J_{\parallel})(\gamma_{15}/\gamma_{14})$	1
	$3  A(14-15)  - \frac{1}{2}(2d - J_{\parallel})(\gamma_{15}/\gamma_{14})$	1

## 2. Intermolecular Interactions

Intermolecular interactions contribute to the width of the component lines of the spectra. Usually, in NQR, linewidths may be attributed to one or more of three causes: (i) magnetic dipole-dipole broadening, (ii) crystalline defects, and (iii) lifetime broadening. For  $\alpha$ -nitrogen  $T_1$  is not short enough to produce significant lifetime broadening.<sup>23</sup> At least two other mechanisms may conceivably produce broadening in  $\alpha$ -nitrogen. These are a possible minor inequivalence of nuclear sites due to the  $P2_13$  structure, and a dynamically induced asymmetry in the electric field gradient (EFG) arising from anharmonicity of the lattice vibrations (see Sec. IV). Additionally, it should be mentioned that anomalies in specific heat and thermal expansion of  $\alpha$ -nitrogen have led some authors<sup>19,33</sup> to postulate that thermally activated orientational defects occur and become appreciable above about 24 K. The evidence for these defects is not conclusive at this time, but if they do occur they should affect the linewidth at higher temperatures. An experiment that may resolve this question is in progress in our laboratory.

The second moment due to dipolar broadening is given in terms of traces of operators by<sup>34</sup>

$$\langle \Delta\nu^2 \rangle = - \frac{\text{Tr}[\bar{\mathcal{H}}_d \bar{\mathcal{H}}_{rf}]^2}{h^2 \text{Tr}(\bar{\mathcal{H}}_{rf})^2}, \quad (6)$$

where  $\bar{\mathcal{H}}_d$  and  $\bar{\mathcal{H}}_{rf}$  are the properly truncated dipolar and radio-frequency Hamiltonians. The two-particle interaction  $\bar{\mathcal{H}}_d$  connects only product states of the main Hamiltonian  $\bar{\mathcal{H}}_Q$  that have the same unperturbed energy, while  $\bar{\mathcal{H}}_{rf}$  induces only transitions that contribute to the main line. If the quadrupole couplings of interacting nuclei differ appreciably, the number of terms to be retained is reduced further. Analogous to dipolar broadening in NMR,

interactions among resonant nuclei broaden the lines more than interactions between resonant and nonresonant nuclei. Thus, the intermolecular second moment for the NQR of  $^{14}\text{N}$  in a  $^{14}\text{N}$ - $^{15}\text{N}$  molecule placed in a pure  $^{14}\text{N}_2$  lattice is expected to be less than that for a  $^{14}\text{N}$ - $^{14}\text{N}$  molecule in the same environment.

Abraham and Kambe<sup>35</sup> have given a formula for the second moment of dipolar broadened NQR lines for spin-1 nuclei that experience identical axially symmetric EFG and interact with other resonant or nonresonant nuclei of arbitrary spin. Their procedure must be generalized for  $\alpha$ -nitrogen to account for the four distinct orientations of the molecules. This can be done by expressing the two-particle interactions in terms of the cubic axes system of the crystal, calculating the necessary matrix elements in the representation of the new eigenvectors of  $\mathcal{H}_Q$ , and appropriately truncating the operators  $\mathcal{H}_d$  and  $\mathcal{H}_{rf}$  using a complete set of matrices for spin 1. This calculation has been performed,<sup>36</sup> but no details will be given here because the derivation is exceedingly tedious and, furthermore, it is concluded that the experimental second moment is not set by the dipolar interactions. The resulting formula was used to calculate the numerical value of the intermolecular second moment out to nuclei in second-nearest-neighbor molecules for the  $P\alpha 3$  crystal structure and a lattice constant of 5.65 Å. The value thus obtained for a powder sample is

$$\langle \Delta\nu^2 \rangle_{\text{inter}} = 1.0 \times 10^4 \text{ Hz.}$$

Thus, one expects a linewidth on the order of 100 Hz. The result would not be significantly different for the  $P2_13$  structure and the considerable extra labor required for the calculation was considered unnecessary.

## B. Discussion of Experimental Spectra for a Normal Isotopic Abundance Sample

Earlier NQR experiments<sup>21,22</sup> on  $\alpha$ -nitrogen yielded a broad ( $\sim 3$  kHz) single line with only a slight indication of structure. Failure to resolve the theoretically predicted intramolecular dipolar splittings was attributed to inhomogeneous broadening caused by the crystallographic disruption occurring at the  $\beta$ - $\alpha$  phase transition. As we have reported recently,<sup>24-27</sup> however, well-resolved spectra can be obtained if the sample is carefully prepared and annealed.

A derivative recording of the NQR spectrum in an annealed sample of natural abundance  $\alpha$ -nitrogen at 4.2 K is shown in Fig. 1. Two sets of lines are observed: a strong asymmetric triplet with approximate amplitude ratios 1:3:2 in order of increasing frequency and a weak doublet (greatly enhanced in Fig. 1) at a higher frequency. On the basis of

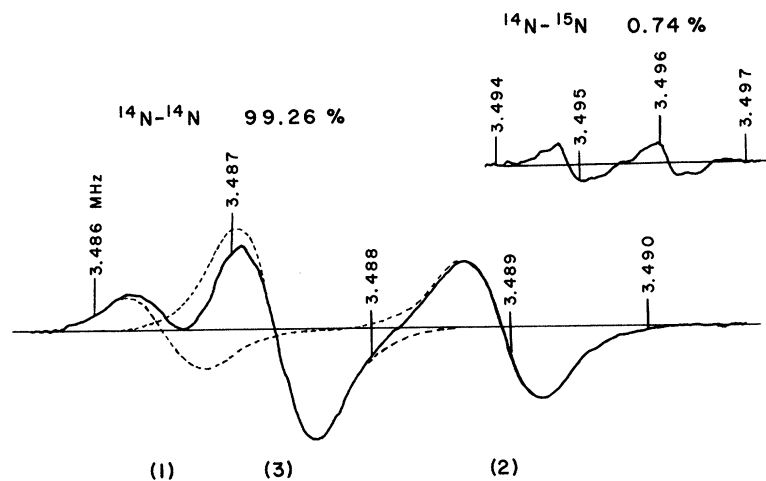


FIG. 1. NQR of  $^{14}\text{N}$  in a natural isotopic abundance (0.37%  $^{15}\text{N}$ ) sample of solid  $\alpha$ -nitrogen at 4.2 K. First-derivative recordings of spectra are shown for the two molecular species  $^{14}\text{N}$ - $^{14}\text{N}$  and  $^{14}\text{N}$ - $^{15}\text{N}$ . Intramolecular dipolar interaction produces a triplet spectrum with intensity ratios 1:3:2 for the symmetric molecule and a doublet for the mixed molecule. Dashed curves indicate the overlapping components of the triplet. Frequency markers are in MHz. The spectrometer gain is much higher for the weak doublet.

relative intensity and theoretically expected structure, the triplet is assigned to the  $^{14}\text{N}$ - $^{14}\text{N}$  molecules (99.26%) and the doublet to the  $^{14}\text{N}$ - $^{15}\text{N}$  molecules (0.74%). From the sense of the asymmetry of the triplet it follows immediately that the quadrupole coupling constant is negative. The nuclear quadrupole moment  $eQ$  is known to be positive and thus the principal value of the electric field gradient  $eq$  is negative, which is in agreement with theoretical calculations.<sup>37</sup>

Because the high-frequency half of the intensity 2 transition of the triplet appears not to overlap with other lines, the spectrum can be unfolded self-consistently (on the assumption that the halves of the derivative lines are antisymmetric) to yield all three components, as illustrated in Fig. 1. Data thus obtained from an average of ten good spectra are given in Table II. This procedure tends to accumulate error, and therefore estimated errors increase in the order that curves are separated. All three curves have approximately the same line-width at half-height of about 720 Hz, as compared to a total width of the spectrum of about 3 kHz. Second moments computed for the lines of intensity 2 and 3 agree within experimental error. The experimental second moments, however, are an order of magnitude greater than the calculated intermolecular dipolar contribution. It seems most probable that the excess broadening arises from residual crystalline strains after the annealing procedure. The experimental line shape is intermediate between Gaussian and Lorentzian, but somewhat closer to the former. One other possible broadening mechanism previously mentioned is a dynamically induced asymmetry in the EFG. An upper limit on the dynamic asymmetry parameter can be set on the basis that the splitting  $\Delta\nu = \frac{2}{3}\nu_Q\eta$  that would result is unresolved. This means that  $\Delta\nu$  must be less than roughly the half width of the reso-

nance line, which leads to the inequality  $\eta(4.2\text{ K}) \leq 1.6 \times 10^{-4}$ .

The small signal-to-noise ratio for the  $^{14}\text{N}$ - $^{15}\text{N}$  resonance precludes detailed analysis. The two component curves do not appear to overlap significantly. The center frequency is determined to have the value  $\nu_Q = 3495.6 \pm 0.1$  kHz and the doublet splitting is  $1200 \pm 40$  Hz. The peak-to-peak separation in the derivative of each line is only about 60% of the value for the  $^{14}\text{N}$ - $^{14}\text{N}$  lines. A reduction in the second moment is expected from the dipolar contribution because the host  $^{14}\text{N}$ - $^{14}\text{N}$  molecules are nonresonant with the  $^{14}\text{N}$ - $^{15}\text{N}$ . However, it was not possible to check this quantitatively. Although isotopically enriched samples were studied that gave good signal-to-noise ratios for the  $^{14}\text{N}$ - $^{15}\text{N}$  molecules, the lines in this case are broadened markedly for additional reasons to be discussed in Sec. V.

A thorough study of the temperature dependence of linewidths in a well-annealed sample has not been made, but recordings of partially annealed samples show that considerable broadening and loss of resolution occur starting above about 15 K and increase with increasing temperature. This broadening is reproducible at any given temperature when the temperature is cycled; thus, it seems to be a ther-

TABLE II. Data for the three components in the  $^{14}\text{N}$ - $^{14}\text{N}$  NQR spectrum at  $T = 4.2$  K, obtained from an average of 10 well-resolved spectra.

Relative amplitude	Center frequency (Hz)	Linewidth at half-height (Hz)	Second moment ( $10^5$ Hz <sup>2</sup> )
$12.9 \pm 0.2$	$3488940 \pm 10$	$720 \pm 20$	$1.24 \pm 0.12$
$20.1 \pm 0.4$	$3487320 \pm 10$	$740 \pm 30$	$1.60 \pm 0.24$
$6.3 \pm 0.3$	$3486510 \pm 20$	$680 \pm 40$	

mal effect.

Although the indirect spin-spin interaction has been included in the Hamiltonians of Eqs. (4) and (5), it is expected to be much weaker than the dipolar perturbation. The static value of the dipolar coupling constant  $d_0$  may be calculated from the known magnetic moment and the nuclear separation  $r_{12} = 1.100 \pm 0.005 \text{ \AA}$ , as determined by spectroscopy.<sup>38</sup> One obtains

$$d_0(14-14) = 471 \pm 6 \text{ Hz.}$$

The value of the  $J$  coupling is not known, but all indications are that the coupling is very small.<sup>39,40</sup>

Thus, to an excellent approximation we may ignore  $J$  and analyze the spectra as pure dipolar splittings.<sup>41</sup> The splitting between the two outer lines [labeled in Fig. 1 according to intensity as (1) and (2)] of the  $^{14}\text{N}$ - $^{14}\text{N}$  spectrum is given by  $\Delta(14-14) = 6d(14-14) = 2430 \pm 30 \text{ Hz}$ , from which it follows that the value of the dipole coupling is

$$d(14-14) = 405 \pm 5 \text{ Hz.}$$

This value is significantly less than the static coupling  $d_0$ , to which it bears the ratio  $f_d(4.2 \text{ K}) = 0.86 \pm 0.02$ . We shall show later that this reduction is accurately explained as an averaging of the dipolar interaction by molecular librations. Within experimental error the same averaging factor is obtained for the doublet spectrum of the  $^{14}\text{N}$ - $^{15}\text{N}$  molecules.

The unperturbed resonance frequency  $\nu_Q(14-14) = 3|A|$  is given by

$$\nu_Q(14-14) = \nu(2) - 3d = 3487.73 \pm 0.03 \text{ kHz,}$$

where  $\nu(2)$  is the frequency of the high-frequency line of intensity 2. This is the best experimental value of the NQR frequency at 4.2 K. Previously reported pulse NQR experiments and continuous wave (cw) experiments with Zeeman modulation measured the position of maximum amplitude of the total absorption curve, and as expected the value of the resonance frequency obtained,  $\nu_Q = 3487.3 \pm 0.1 \text{ kHz}$ , corresponds almost exactly to the center of line (3).

We have also attempted to include  $J_\perp$  and  $J_\parallel$  in the analysis of the splittings and to deduce values for these parameters. The details will not be given because the calculation is involved and the results, as expected, are not very reliable. The value of  $d$  is unchanged, and for the  $J$ -coupling parameter  $J = \frac{1}{3}(2J_\perp + J_\parallel)$  we obtain  $J(14-14) = -46 \pm 39 \text{ Hz}$  and  $J(15-15) = -90 \pm 76 \text{ Hz}$ . The range of error makes the numerical value almost meaningless, but the preference for a negative sign may be significant. We are presently using spin-echo techniques, which are not affected by inhomogeneity broadening, in an effort to improve on these data.

#### IV. TEMPERATURE AND VOLUME DEPENDENCE OF RESONANCE FREQUENCIES

##### A. Theoretical Background

The temperature dependence of nuclear quadrupole resonance frequencies, either under the condition of constant pressure or constant volume, is caused by thermal excitation of lattice vibrations. The maximum principal component of the EFG tensor and the asymmetry parameter expressed as appropriate thermal averages are given by

$$eq(T) = \langle V_{zz} \rangle, \quad (7)$$

$$\eta(T) = (\langle V_{xx} \rangle - \langle V_{yy} \rangle) / \langle V_{zz} \rangle. \quad (8)$$

A general theory for the temperature dependence of the EFG tensor, allowing for an anharmonic potential and including dispersion in the vibration spectrum, has not yet been developed. Fortunately, the complexity of the problem is reduced by the fact that not all vibrations contribute significantly to the temperature dependence in actual cases studied. In molecular solids, for example, where the EFG is chiefly of intramolecular origin, the most effective vibrations in averaging are usually the librations. In the simplest theoretical model it is assumed that the potential is harmonic and that the molecule librates as a rigid body. The effect of a single libration on the nuclear quadrupole coupling constant was first treated in this manner by Bayer<sup>42</sup> and the theory was later generalized by Kushida<sup>43</sup> to include all normal modes.

For a linear molecule such as  $\text{N}_2$ , executing rapid rigid-body harmonic librations, the averaging of the intramolecular EFG is given by<sup>44</sup>

$$q(T) = q' \left( -\frac{1}{2} + \frac{3}{2} \langle \cos^2 \theta_y \rangle \langle \cos^2 \theta_x \rangle \right), \quad (9)$$

$$\eta(T) = [3q'/2q(T)] | \langle \cos^2 \theta_x \rangle - \langle \cos^2 \theta_y \rangle |. \quad (10)$$

Here,  $\theta_x$  and  $\theta_y$  are angular amplitudes about the  $x$  and  $y$  axes and  $q'$  is the principal component of EFG averaged over all vibrations of the molecule *other than* the librations. The static asymmetry parameter of a linear molecule is zero, but the dynamic asymmetry parameter is not if the motion is anisotropic. Usually it is assumed that the angular amplitudes are small and the cosine functions in Eqs. (9) and (10) are expanded. For  $\alpha$ -nitrogen it is necessary to retain terms to the sixth order in angle and we obtain

$$q(T) \approx q' \left[ 1 - \frac{3}{2} (\langle \theta_x^2 \rangle + \langle \theta_y^2 \rangle) + \frac{1}{2} (\langle \theta_x^4 \rangle + \langle \theta_y^4 \rangle) + \frac{3}{2} \langle \theta_x^2 \rangle \langle \theta_y^2 \rangle - \frac{1}{15} (\langle \theta_x^6 \rangle + \langle \theta_y^6 \rangle) - \frac{1}{2} (\langle \theta_x^2 \rangle \langle \theta_y^4 \rangle + \langle \theta_x^4 \rangle \langle \theta_y^2 \rangle) \right], \quad (11)$$

$$\eta(T) \approx [q'/q(T)] \left[ -\frac{3}{2} (\langle \theta_x^2 \rangle - \langle \theta_y^2 \rangle) + \frac{1}{2} (\langle \theta_x^4 \rangle - \langle \theta_y^4 \rangle) - \frac{1}{15} (\langle \theta_x^6 \rangle - \langle \theta_y^6 \rangle) \right]. \quad (12)$$

In the harmonic approximation, the angular ampli-

tudes  $\theta_i$  may be expanded in terms of the normal coordinates  $Q_i$ , and averages of  $\theta_i^m$  are given by

$$\langle \theta_i^m \rangle = \sum_{n \dots l} C_{in} \dots C_{il} \langle Q_n \dots Q_l \rangle, \quad (13)$$

where  $C_{ij}$  are expansion coefficients. Averages of the normal coordinates may be calculated using quantum statistical mechanics and then related to  $\langle \theta_i^m \rangle$  via Eq. (13) and the symmetry properties of the crystal lattice. For the *Pa3* structure it may be shown that

$$\langle \theta_x^{2m} \rangle = \langle \theta_y^{2m} \rangle \equiv \langle \theta^{2m} \rangle, \quad m = 1, 2, \dots \quad (14)$$

Consequently, for  $\alpha$ -nitrogen, the dynamic asymmetry parameter is zero and Eq. (11) reduces to

$$q(T) = q'(1 - 3 \langle \theta^2 \rangle + \langle \theta^4 \rangle + \frac{3}{2} \langle \theta^2 \rangle^2 - \frac{2}{15} \langle \theta^6 \rangle - \langle \theta^2 \rangle \langle \theta^4 \rangle) \\ \equiv q' f_i(T), \quad (15)$$

where  $f_i(T)$  is the librational averaging factor. The mean-square amplitude of a harmonic oscillator is related to temperature by the expression<sup>6</sup>

$$\langle \theta^2 \rangle = (h/8 \pi^2 nI) \sum_i (g_i/\nu_i) \coth(h\nu_i/2kT), \quad (16)$$

where  $n$  is the number of librational degrees of freedom of the basis,  $g_i$  is the degeneracy of the normal-mode frequency  $\nu_i$ , and  $I$  is the moment of inertia of the molecule. Similarly, we have

$$\langle \theta^4 \rangle = 3 \langle \theta^2 \rangle^2, \quad (17)$$

$$\langle \theta^6 \rangle = 15 \langle \theta^2 \rangle^3. \quad (18)$$

Using Eqs. (17) and (18), the librational averaging factor simplifies to

$$f_i(T) = [1 - 3 \langle \theta^2 \rangle + \frac{9}{2} \langle \theta^2 \rangle^2 - 5 \langle \theta^2 \rangle^3]. \quad (19)$$

The quadrupole resonance frequency is given by

$$\nu_Q = \nu'_0 f_i(T), \quad (20)$$

where for spin-1 nuclei  $\nu'_0 = 3e^2 Qq'/4h$ . It may also be shown<sup>36</sup> that the intramolecular magnetic dipole-dipole interaction should be averaged by the librations to the same extent as is  $\nu_Q$ ; i. e.,  $d(T) = d'_0 f_i(T)$ .

In the quasiharmonic approximation one attempts to account for the actual anharmonic potential, including effects of thermal expansion, within the framework of the harmonic theory by allowing the  $\nu_i$  in Eq. (16) to be functions of temperature. Two approaches are possible in analyzing NQR data. If through independent spectroscopic measurements the true temperature dependences of the  $\nu_i$  are known, these may be used directly and theory compared with experiment. Agreement is not expected to be perfect because the harmonic equations do not describe the eigenstates of the real solid. Alternatively, one may fit Eq. (20) to experimental NQR data using the  $\nu_i$  as adjustable parameters. The temperature dependence of the  $\nu_i$  obtained in

this way will not be the true temperature dependence and one must be wary of giving it physical meaning, as has sometimes been done in the literature, because erroneous conclusions may be reached.

Additional factors must, in general, be included in the theory of real solids. As noted,  $q'$  in Eq. (9) includes the effect of all the vibrations other than the librations. We may write

$$q' = q_0 f', \quad (21)$$

where  $f'$  measures the averaging by other motions and  $q_0$  is the static-field gradient. Then we have

$$q(T) = f_Q q_0, \quad (22)$$

where

$$f_Q = f' f_i. \quad (23)$$

It must be recognized that  $q_0$  and even the moment of inertia  $I$  appearing in Eq. (16) are potentially functions of volume and thus may change during constant pressure experiments. This problem has been discussed phenomenologically by Kushida, Benedek, and Bloembergen,<sup>45</sup> and by Gutowsky and Williams,<sup>46</sup> who show that the effects may be separated by a detailed temperature and volume study.

In all cases that have been reported to date the equation of state of the material is inadequately known for detailed and accurate analysis. Fortunately, solid  $\alpha$ -nitrogen, because of the simplicity and convenient properties of the molecule and crystal structure, is free of much of the bothersome complexity encountered in other solids. Furthermore, complete thermodynamic and spectroscopic data on nitrogen are now available, permitting for the first time an extensive study of the NQR data.

## B. Experimental Results and Discussion

### 1. Resonance Frequency

The pressure dependence of the resonance frequency of  $^{14}\text{N}$  in  $^{14}\text{N}$ - $^{14}\text{N}$  molecules in a natural abundance sample of  $\alpha$ -nitrogen is shown in Fig. 2 for seven temperatures. The termination of each curve is set by fusion of the fluid helium pressure transmitting medium at that temperature. The experimental method is described in Sec. II.

The pressure dependence of the resonance frequency  $\nu_Q$  is a remarkably strong function of temperature near the phase transition. Initial slopes  $(\partial \nu_Q / \partial P)_0$  are shown vs temperature in Fig. 3. At 35 K, the highest temperature for which data were taken, a pressure change of only 1 bar shifts  $\nu_Q$  by 300 Hz (almost the linewidth)! This fact is striking evidence for a dynamic instability critically dependent upon volume.

The dashed curve in Fig. 2 indicates the pressure required at each temperature to compress the sam-

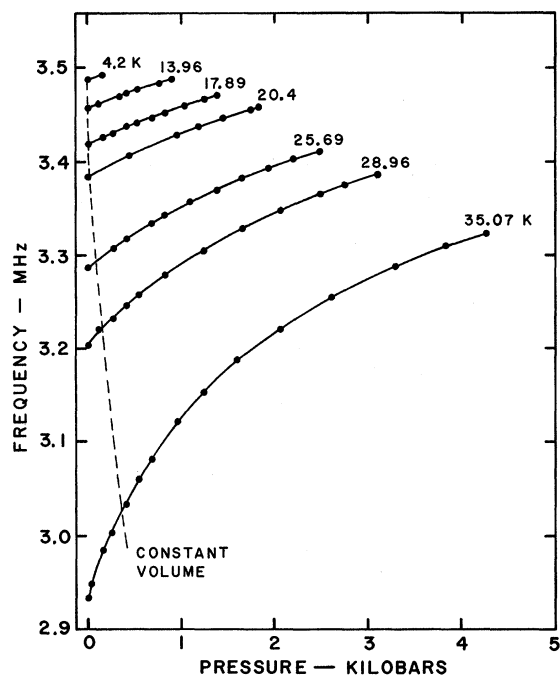


FIG. 2. NQR frequency  $\nu_Q$  of  $^{14}\text{N}$  in  $^{14}\text{N}$ - $^{14}\text{N}$  molecules in a natural isotopic abundance sample of  $\alpha$ -nitrogen as a function of hydrostatic pressure at seven fixed temperatures. The intersection of the dashed curve with the solid curves marks the resonance frequency at constant volume  $V(0)$ , the volume at  $T=0$  K and  $P=0$ . For clarity, the scale on the left-hand side is offset from  $P=0$ .

ple to its initial volume at 4.2 K (essentially 0 K). The intersections of this curve with the isotherms give the resonance frequency as a function of temperature at constant volume. The dashed curve was

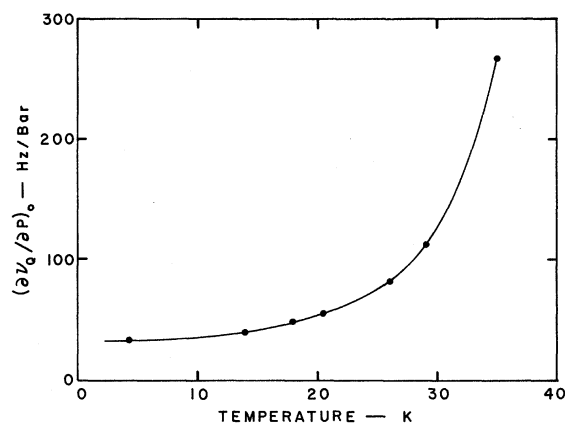


FIG. 3. Temperature dependence of the initial (zero pressure) slopes  $(\partial\nu_Q/\partial P)_0$  obtained from Fig. 2.

calculated from thermal expansion and compressibility data.<sup>17</sup> Except near the phase transition, the pressure required to maintain constant volume is so low that the pressure dependence of the compressibility may be ignored and the required pressure calculated from the relation

$$\Delta P = - (1/\chi)(\Delta V/V), \quad (24)$$

where  $\chi$  is the initial compressibility and  $\Delta V$  is the volume thermal expansion. Recently, at our suggestion, Anderson and Swenson<sup>29</sup> measured  $V/V_0$  vs  $P$  for  $\alpha$ -nitrogen at several temperatures and fit their data with the Murnaghan equation of state.<sup>47</sup> These data have been used to refine the constant volume curve to include the variation of compressibility with pressure.

The normalized temperature dependence of the

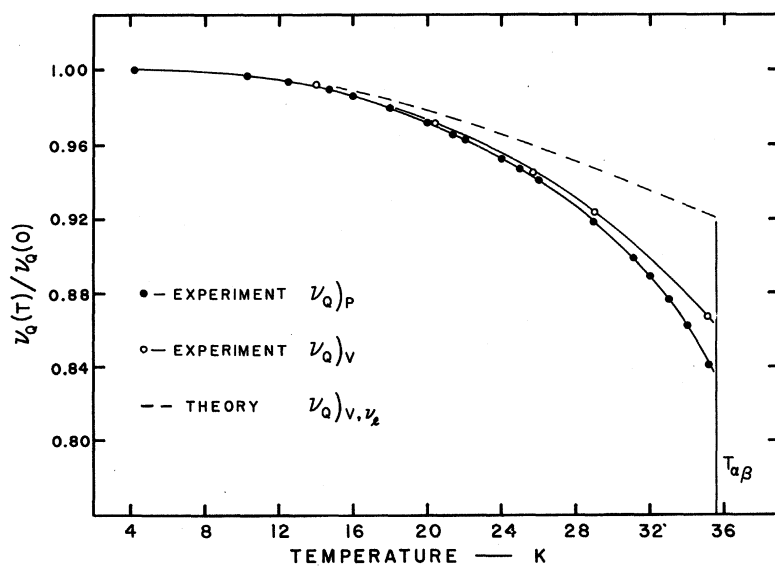


FIG. 4. Temperature dependence of the reduced NQR frequency  $\nu_Q(T)/\nu_Q(0)$  of  $^{14}\text{N}$  in  $^{14}\text{N}$ - $^{14}\text{N}$  molecules in a natural isotopic abundance sample of  $\alpha$ -nitrogen. The solid circles are experimental data at zero pressure. Open circles represent experimental results at constant volume  $V(0)$ , the equilibrium volume at zero temperature and pressure. The dashed curve is a theoretical temperature dependence at constant volume  $V(0)$  calculated by assuming harmonic librations at frequencies given in Ref. 7.

TABLE III. Libration frequencies at the zone center in units of  $\text{cm}^{-1}$  measured by Raman spectroscopy. The numbers in parentheses are the linewidths at half-height. The temperature for the measurement is indicated in parentheses beside the author identification.

BRS <sup>a</sup> (12 K)	CL <sup>b</sup> (16 K)	ASD <sup>c</sup> (18 K)
31.5(1.4)	33.5(1.6)	32 (1.5)
35.8(1.4)	37.5(1.6)	36.5(1.5)
		60 (4)

<sup>a</sup>Reference 5.

<sup>b</sup>Reference 6.

<sup>c</sup>Reference 7.

resonance frequency [ $\nu_Q(T)/\nu_Q(0) = f_Q$ ] at constant zero pressure and at constant volume are shown in Fig. 4. It is seen that correcting for thermal expansion makes relatively little difference in the strong temperature variation, which must therefore be attributed to thermal excitations. We now turn to a review of what is known about lattice dynamics of  $\alpha$ -nitrogen.

## 2 Lattice Dynamics of $\alpha$ -Nitrogen

Because the EFG is almost completely intramolecular in origin, the NQR temperature dependence is strongly dominated by the librations. The open structure of  $\alpha$ -nitrogen and the molecular rigidity preclude significant dynamic distortion of the molecules. For this reason, translations, even though they are of low energy and readily excited, can directly affect only the intermolecular EFG. The stretching mode does directly modify the intramolecular EFG, and this has a small effect on the ground-state averaging factor. However, the effect of the stretching mode on the temperature dependence of  $\nu_Q$  is negligible because the stretching frequency<sup>6</sup> is so high (2329  $\text{cm}^{-1}$  or 3348 K) that the molecules are not significantly excited out of the ground state for temperatures in the  $\alpha$ -phase.

A group-theoretical analysis<sup>28</sup> of the lattice vibration problem predicts that the eight zone-center librations of the  $Pa3$  structure are distributed among two triply degenerate  $T_g$  modes and one doubly degenerate  $E_g$  mode. For the correct  $P2_13$  structure these degeneracies are not modified but mixing with translational modes is allowed. There is no evidence, however, from infrared and Raman spectra that such mixing occurs, and it is evidently very weak and of no consequence for our discussion of the NQR data. Four independent Raman spectroscopy experiments<sup>5-7,48</sup> have recently been conducted from which the libration frequencies at the zone center ( $\vec{k} = 0$ ) were obtained. Published data are summarized in Table III. Only two Raman frequencies were observed by Brith, Ron, and Schnepp<sup>5</sup> (BRS), and by Cahill and Leroi<sup>6</sup> (CL); it was postulated by these authors that the  $E_g$  and one

of the  $T_g$  modes are accidentally degenerate. This hypothesis was supported by intensity measurements and a theoretical calculation<sup>13,14</sup> of the frequencies using an atom-atom potential with three adjustable parameters. Anderson, Sun, and Donkersloot<sup>7</sup> (ASD) find, in addition to the two low-frequency lines, a third line at 60  $\text{cm}^{-1}$  which they assign to the missing  $T_g$  vibration. A theoretical calculation of frequencies and intensity ratios using the molecular quadrupole-quadrupole orientational potential with the quadrupole moment as an adjustable parameter yields excellent agreement with the ASD experimental results. Although it is possible that the weak line at 60  $\text{cm}^{-1}$  is an overtone of the strong line at 32  $\text{cm}^{-1}$ , the assignment as a fundamental yields a frequency set that is more consistent with patterns of relative frequencies and intensities that are observed in other molecular crystals ( $\text{CO}_2$  and  $\text{N}_2\text{O}$ ) of the same symmetry and type of orientational interactions. The high-frequency line has also been observed by Mathai and Allin.<sup>48</sup>

The Raman spectra have been observed at several temperatures at zero pressure. All the lines broaden substantially with increasing temperature and the frequency of the most intense line at 32  $\text{cm}^{-1}$  is found to decrease above about 20 K and to soften markedly near  $T_{\alpha\beta}$ . Unfortunately, for the other lines a low intensity compounded by broadening prevented measurement of the temperature dependence of the frequency. We therefore make the simple assumption that all the lines are temperature dependent in proportion to their frequency, that is,

$$\nu_{ii}(T)/\nu_{ii}(0) = \nu_{ii}(T)/\nu_{ii}(0) .$$

This scaling condition is found to be approximately true for the lattice frequencies of carbon dioxide<sup>6</sup> which has the  $Pa3$  crystal structure. The exact behavior is not critical for our argument.

Having a complete set of Raman frequencies we can calculate the librational averaging factor from Eqs. (16) and (19). It is important to note that the libration energies are low (32  $\text{cm}^{-1} = 48$  K) and appreciable excitation must occur in the  $\alpha$ -phase. A simple calculation shows that excitation becomes significant above about 20 K, and that near  $T_{\alpha\beta}$  more than one-quarter of the molecules are in excited states. Anomalous behavior in specific heat, thermal expansion, and compressibility that have been observed above 20 K are to be ascribed to thermal excitation of librations, and the  $\alpha$ - $\beta$  phase transformation undoubtedly results from instability of the structure against increasing reorientations.

## 3. Nuclear Quadrupole Coupling Constant in the Absence of Librations

The NQR frequency at 4.2 K is  $3.48773 \pm 0.00003$  MHz. The internuclear separation  $r_{12}$  within a

TABLE IV. Librational averaging factor  $f_l(4.2 \text{ K})$  calculated for each set of published Raman frequencies. The corresponding resonance frequency  $\nu'_0 = \nu_Q(4.2 \text{ K})/f_l(4.2 \text{ K})$  and coupling constant  $(e^2qQ/h)'_0 = 4\nu'_0/3$  are listed for  $^{14}\text{N}$ - $^{14}\text{N}$  molecules in the absence of librations. An error of  $1.5 \text{ cm}^{-1}$  is allowed for each libration frequency in the calculations.

Reference	Libration frequencies ( $\text{cm}^{-1}$ )	$f_l(4.2 \text{ K})$	$\nu'_0$ (MHz)	$(e^2qQ/h)'_0$ (MHz)
BRS <sup>a</sup>	{31.5, 31.5, 35.8}	$0.836 \pm 0.004$	$4.17 \pm 0.02$	$5.56 \pm 0.03$
CL <sup>b</sup>	{33.5, 33.5, 37.5}	$0.844 \pm 0.004$	$4.13 \pm 0.02$	$5.50 \pm 0.03$
ASD <sup>c</sup>	{32, 36.5, 60}	$0.866 \pm 0.004$	$4.03 \pm 0.02$	$5.37 \pm 0.03$

<sup>a</sup>Reference 5.

<sup>b</sup>Reference 6.

<sup>c</sup>Reference 7.

molecule is taken to be  $1.100 \pm 0.005 \text{ \AA}$ , yielding a range in moment of inertia of  $1.405 \leq I \leq 1.430 \times 10^{-39} \text{ g cm}^2$ . The librational averaging factor  $f_l(4.2 \text{ K})$  calculated for each set of published Raman frequencies is given in Table IV together with the corresponding resonance frequency  $\nu'_0 = \nu_Q(T)/f_l(T)$  and coupling constant  $(e^2qQ/h)'_0 = \frac{4}{3}\nu'_0$  in the absence of librations. Because the stretching frequency is virtually unchanged from solid to gas, this value of the coupling constant should be close to that for the free molecule, which has not yet been measured.

#### 4. Averaging of the Intramolecular Dipolar Splitting

The librational averaging factor just computed is identical, within experimental error, with the averaging factor  $f_d$  found independently from the dipolar splitting of the spectrum.<sup>49</sup> This result shows that librations are the operating mechanism in the dipolar averaging at 4.2 K. Furthermore, the agreement provides a test of the assumption of rigid-body harmonic librations that has been made for the calculation  $f_l$ . It is important to note that the averaging of the dipolar interaction and of the quadrupole coupling constant are physically rather different processes and need not be given by the same factor. Whereas the dipolar interaction is between two point nuclei embedded deeply within the molecule, the quadrupole interaction involves the entire charge cloud of the molecule and is much more susceptible to perturbation in the solid. Furthermore, the time scales involved for averaging differ by three orders of magnitude. Spin-echo work currently in progress in our laboratory shows that the two averaging factors are identical to within 0.2% at all temperatures.<sup>50</sup>

#### 5. Analysis of the Temperature Dependence of the Resonance Frequency

It is informative first to compare the temperature dependence of  $\nu_Q$  at constant volume with the theoretical curve obtained using the values of the libration frequencies measured at low temperature. If the Raman frequencies were functions only of volume then these two curves should agree rea-

sonably well. The comparison is made in Fig. 4. The experimental constant volume temperature dependence is substantially stronger than the theoretical variation. The explanation of this discrepancy is that the harmonic model on which Eqs. (16) and (19) are based is inadequate at higher temperatures for  $\alpha$ -nitrogen. The libration frequencies evidently have an intrinsic temperature dependence that is due to anharmonicity of the orientational potential (which may itself be a function of the number of excitations). Quasiharmonic theory, in fact, is much more successful in explaining experiment. In Fig. 5 we compare the experimental temperature dependence of  $\nu_Q$  at constant pressure with theoretical curves obtained using the experimentally observed Raman frequencies. The temperature dependence of the libration frequencies is estimated from the CL and BRS measurements at several temperatures of the lowest frequency, assuming that the ratios of the three frequencies remain at their low-temperature values. Three theoretical curves are shown; one each for the CL and BRS frequencies (assuming an accidental degeneracy) and the third for the ASD frequencies but with the BRS temperature dependence. It is evident that in all cases the agreement is fairly good and much better than for the constant volume harmonic theory.

Comparison of the experimental curve in Fig. 5 with the theoretical curves shows that the CL frequencies give best over-all agreement. The BRS frequencies overestimate the temperature dependence of  $\nu_Q$  even at low temperature, which implies that on the whole the frequencies are too low. The ASD or MA assignment underestimates the temperature dependence of  $\nu_Q$ , although lowering the values of the libration frequencies to 30, 34, and  $56 \text{ cm}^{-1}$  is sufficient to obtain agreement below 20 K. Some underestimation of the temperature dependence, especially at higher temperatures, may be expected because other modes that are being ignored may make small contributions to the experimental averaging, although we have argued that this should not be much in nitrogen.

The primary conclusion to be drawn from Fig. 5 is that the quasiharmonic theory is rather success-

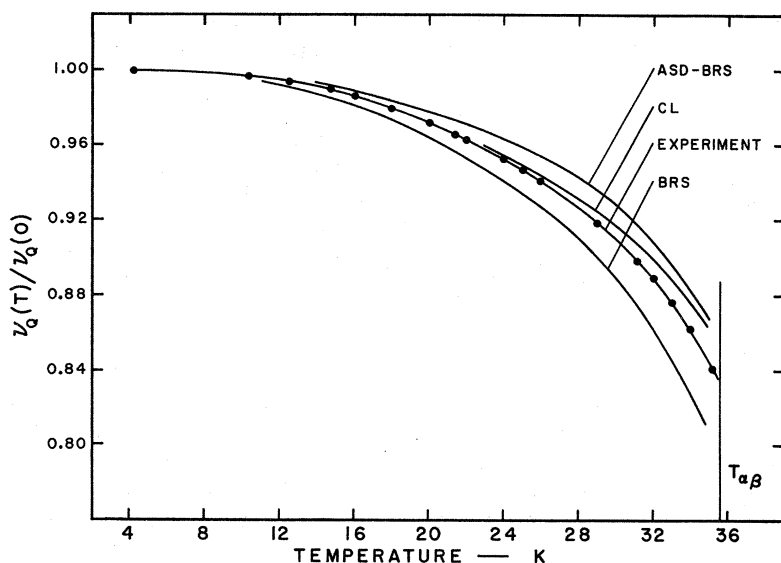


FIG. 5. Temperature dependence of the reduced NQR frequency  $\nu_Q(T)/\nu_Q(0)$  of  $^{14}\text{N}$  in  $^{14}\text{N}-^{14}\text{N}$  molecules in a natural isotopic abundance sample of  $\alpha$ -nitrogen at zero applied pressure. Experimental data, shown by solid circles, are compared with theoretical calculations of motional averaging produced by thermal excitation of anharmonic molecular librations. The temperature variation is calculated for each of three sets of published Raman frequencies: ASD (Ref. 7), CL (Ref. 6), and BRS (Ref. 5). For clarity, the theoretical curves are not shown in regions where they merge with the experimental curves.

ful in explaining the strong temperature dependence of  $\nu_Q$ . No adjustable parameters have been used in the theory and there is no fitting except to obtain  $\nu_Q$  at 4.2 K. It may be surmised, therefore, that neglected effects such as dispersion are indeed small in  $\alpha$ -nitrogen. This conclusion is in agreement with the theoretical work of Schnepf and Ron<sup>14</sup> who have calculated dispersion curves for  $\alpha$ -nitrogen and find relatively little dispersion in the librational branches.

#### 6. Volume Dependence of NQR Frequency

Since the equation of state of  $\alpha$ -nitrogen is now known in considerable detail except in the close vicinity of the phase transition, the volume dependence of the quadrupole coupling constant may be deduced from the pressure data of Fig. 2. We have used data on thermal expansion and compressibility obtained in our laboratories<sup>17</sup> together with the PVT work by Anderson and Swenson<sup>29</sup> to calculate the results in Fig. 6. The quadrupole coupling constant is found to be practically a linear function of volume over the volume range for which measurements were made at the lower temperatures, but curvature is increasingly evident at higher pressures and temperatures near the phase transformation. The volume dependence is a strong function of temperature and a curve of the derivatives  $(\partial\nu_Q/\partial V)_T$  vs  $T$  has an appearance very similar to that for the pressure derivatives shown in Fig. 3.

#### 7. Volume Dependence of the Libration Frequencies

Because the averaging of the EFG by the librations gives a good description of the temperature dependence of  $\nu_Q$  it is possible to obtain information about the volume dependence of  $\nu_i$  from the

volume dependence of  $\nu_Q$ . In the harmonic approximation, the libration frequencies are related to the angular force constants  $G_{ij}$  through the secular equation

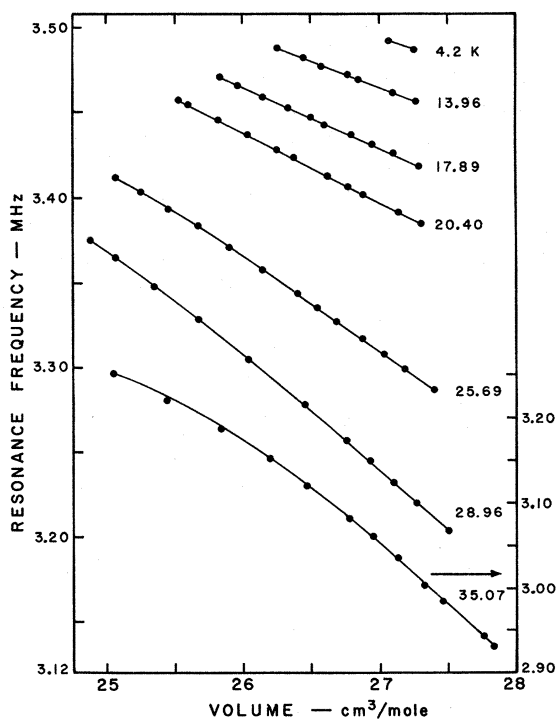


FIG. 6. Volume dependence of the NQR frequency  $\nu_Q$  of  $^{14}\text{N}$  in  $^{14}\text{N}-^{14}\text{N}$  molecules in natural isotopic abundance  $\alpha$ -nitrogen at seven fixed temperatures. Frequency scale for the 35.07-K isotherm is on the right-hand side of the graph; all other curves refer to the scale on the left-hand side.

TABLE V.  $^{14}\text{N}$  NQR frequencies for  $^{14}\text{N}$ - $^{14}\text{N}$  and  $^{14}\text{N}$ - $^{15}\text{N}$  molecules and their difference  $(\Delta\nu)_{\text{isotope}}$  at  $T=4.2$  K in five isotopic mixtures.

Conc. (% $^{15}\text{N}$ )	$\nu_Q(14-15)$ (kHz)	$\nu_Q(14-14)$ (kHz)	$(\Delta\nu)_{\text{isotope}}$ (kHz)
0.37	$3495.6 \pm 0.1$	$3487.7 \pm 0.10$	$7.9 \pm 0.20$
10.0	$3495.9 \pm 0.1$	$3488.0 \pm 0.15$	$7.9 \pm 0.25$
33.0	$3496.4 \pm 0.1$	$3488.5 \pm 0.15$	$7.9 \pm 0.25$
46.8	$3496.4 \pm 0.1$	$3488.4 \pm 0.15$	$8.0 \pm 0.25$
$\sim 99.0$	$3498.3 \pm 0.1$	$3490.3 \pm 0.15$	$8.0 \pm 0.25$

$$|G_{ij} - 4\pi^2 I \nu_i^2 \delta_{ij}| = 0, \quad (25)$$

where  $I$  is the moment of inertia of the molecule. We can expand  $\nu_i(V)$  in a Taylor series about the initial volume  $V_0 = a_0^3$  and obtain to first order

$$\nu_i(V) \approx \nu_{i0} - \nu_{i0} b(\nu_{i0})(1 - V/V_0), \quad (26)$$

where  $\nu_{i0} \equiv \nu_i(V_0)$  and

$$b(\nu_{i0}) = \frac{1}{6} \frac{a_0}{I \nu_{i0}^2} \left( \frac{d(I \nu_i^2)}{da} \right)_{a=a_0}. \quad (27)$$

For the molecular quadrupole-quadrupole orientational potential, all the angular force constants are proportional to  $Q_M^2/a^5$ , where  $a$  is the lattice constant and  $Q_M$  is the molecular quadrupole moment. Therefore, as long as  $Q_M$  is not a function of volume, at a given volume  $V$  the ratio  $\nu_i(V)/\nu_i(V_0)$  is the same for all the libration frequencies and the coefficient  $b(\nu_{i0})$  has the value  $-\frac{5}{6}$ . These results allow a test of the degree to which the molecular quadrupole-quadrupole potential model with constant  $Q_M$  describes librations in  $\alpha$ -nitrogen.

At temperatures below about 20 K where the number of excitations is small, the libration frequencies  $\nu_{i0}$  are practically temperature independent, anharmonic effects are not so important, and equa-

tions derived in the harmonic approximation are reasonably valid. Curves of  $\nu_i(V)$  were generated point by point from the volume dependence of  $\nu_Q$  at the fixed temperatures 13.96, 17.89, and 20.4 K as shown in Fig. 6, by using Eqs. (16), (19), and (20). For these calculations we explored all of the sets of frequencies listed in Table III as well as frequencies that were slightly adjusted to precisely fit Eq. (20) to the experimental  $\nu_Q(T)$  curve below 20 K. In every case linear relations of the form of Eq. (27) were obtained. The magnitudes of the slopes  $b(\nu_{i0})$  obtained for these various cases lie in the range  $1.0 \leq |b(\nu_{i0})| \leq 1.5$  (probable error included). Since these values are larger than  $\frac{5}{6}$  we conclude that the molecular quadrupole-quadrupole potential with constant  $Q_M$  is not a sufficient approximation to the orientational intermolecular potential in  $\alpha$ -nitrogen. In order to account for the volume dependence of the libration frequencies, the orientational potential must be more strongly dependent on volume. This could arise from terms containing higher powers of intermolecular separation, such as a Lennard-Jones potential, or from a dependence of  $Q_M$  on volume. If the effective  $Q_M$  in the solid is subject to dynamic corrections, then a dependence on volume is implied. It has been suggested<sup>9</sup> that an averaging of the effective molecular quadrupole moment may explain the observed decrease in the infrared intensity in  $\alpha$ -nitrogen.

#### V. NQR OF $^{14}\text{N}$ IN ISOTOPIC MIXTURES WITH $^{15}\text{N}$

The resonance frequency of  $^{14}\text{N}$  has been measured at 4.2 K for  $^{14}\text{N}$ - $^{14}\text{N}$  and  $^{14}\text{N}$ - $^{15}\text{N}$  molecules in five isotopic mixtures ranging in concentration from 0.37 to 99%  $^{15}\text{N}$ . These data are given in Table V. Three isotopic mass effects are found. There is first and foremost a difference between the resonance frequencies of the two molecular species that we shall call the isotope splitting. The

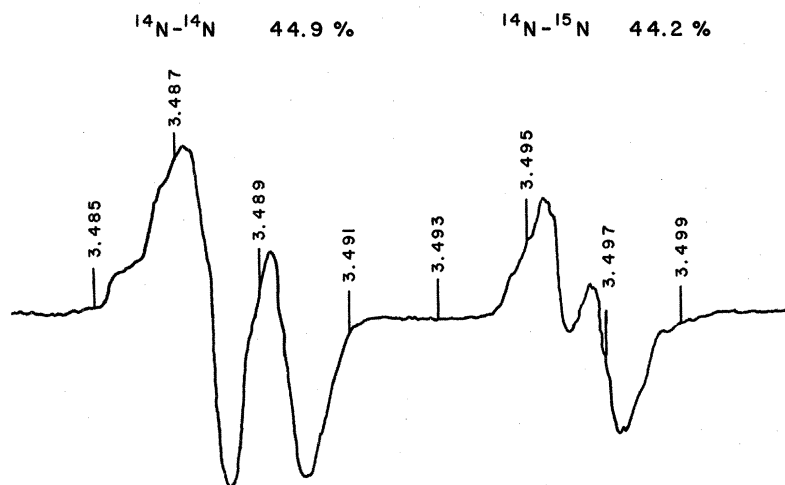


FIG. 7. NQR of  $^{14}\text{N}$  at 4.2 K in a sample of  $\alpha$ -nitrogen isotopically enriched to 33%  $^{15}\text{N}$ . A first-derivative recording of the spectra is shown from a single sweep. The resonance frequency of the mixed molecule is at the higher frequency. Frequency markers are in MHz.

splitting is approximately 8 kHz and is independent of concentration within experimental error. Secondly, the resonance frequency of each molecule is a function of concentration and in both cases increases by almost 3 kHz as the proportion of  $^{15}\text{N}$  is increased from 0.37% to 99%. We shall call this second effect the isotope shift. The shift seems to be approximately a linear function of concentration for the limited number of concentrations studied, although the data on the 46.8% sample deviate from linearity by more than the estimated error. Both these effects were previously observed by Haigh and Scott,<sup>22</sup> but at the time insufficient information was available about solid nitrogen for detailed calculations. The new data presented here are much more precise as well as extensive. As we shall show, the effects provide a sensitive probe of molecular dynamics in lattices with mass defects.

A derivative recording of the spectra of both molecules in the 33%  $^{15}\text{N}$  sample is shown in Fig. 7. A third isotopic effect may be noted on this recording, but it is not unrelated to the shift. Although the sample from which this spectrum was obtained had been carefully annealed, it is readily seen that the resolution is not nearly as good as in Fig. 1. This broadening of the lines was characteristic of all the mixtures between the nearly pure extremes. Clearly it is a consequence of the statistical randomness of the environment of a given type of molecule that must produce a dynamic disorder and local inhomogeneity in the average EFG that cannot be removed by annealing.

#### A. Isotope Shift

The isotope shift may be interpreted simply as a volume effect. The lattice constants of pure  $^{14}\text{N}_2$  and pure  $^{15}\text{N}_2$  have been measured at 20 K and are found to be  $5.660 \pm 0.002$  and  $5.646 \pm 0.002$  Å, respectively.<sup>51</sup> Because relatively little thermal expansion<sup>17</sup> occurs below 20 K, any difference in expansion of the two isotopes should not change the difference in lattice constants significantly from what it is at 20 K. Thus we may take  $\Delta a(4.2\text{K}) = 1.4 \pm 0.4 \times 10^{-2}$  Å. A  $^{14}\text{N}$ - $^{14}\text{N}$  molecule placed in a pure  $^{15}\text{N}_2$  lattice is, in effect, compressed by its environment. We have seen from pressure data in Fig. 2 that compression increases the resonance frequency, which is the sense of the isotope shift. Since the isothermal compressibility of  $\alpha$ -nitrogen is known at 4.2 K ( $\chi = 4.65 \times 10^{-5}$  atm<sup>-1</sup>) we may readily compute the pressure that would be required to compress pure  $^{14}\text{N}_2$  to the volume of pure  $^{15}\text{N}_2$ ; from Eq. (24) it is

$$P = -3\Delta a/a\chi = 1.60 \pm 46 \text{ atm.}$$

From Fig. 3,  $(\partial\nu_Q/\partial P)_{4.2\text{K}} = 33 \pm 3$  Hz/atm, and from this we arrive at a shift of  $5.3 \pm 1.7$  kHz. This number is twice the observed isotope shift of 2.6

$\pm 0.25$  kHz for  $^{14}\text{N}$ - $^{14}\text{N}$  in 99%  $^{15}\text{N}_2$ . That the calculation should overestimate the isotope shift is to be expected because the dynamically larger  $^{14}\text{N}$ - $^{14}\text{N}$  molecule surely reacts by locally expanding the surrounding  $^{15}\text{N}_2$  lattice. Local volume defects associated with mass defects have been considered by several authors, especially in connection with isotopic mixtures of solid helium.<sup>52,53</sup> In general, it is concluded that the local volume defect  $\delta V/V$  is proportional to  $-\delta M/M$  (or some function of this parameter), where  $M + \delta M$  is the mass of the isotopic defect. Thus,  $\delta V$  is positive if the mass is reduced and negative around a larger mass. This reasoning also explains why the isotope shift is the same for the  $^{14}\text{N}$ - $^{15}\text{N}$  and the  $^{14}\text{N}$ - $^{14}\text{N}$  molecule in going from a host lattice of pure  $^{14}\text{N}_2$  to pure  $^{15}\text{N}_2$ , since the net change in mass with respect to the host is the same in both cases. In pure  $^{14}\text{N}_2$  the  $^{14}\text{N}$ - $^{15}\text{N}$  molecule permits the lattice to contract locally, whereas in pure  $^{15}\text{N}_2$  it expands the lattice locally.

From a more definitive viewpoint, the isotope shift must be considered in terms of the vibrations of the defect molecules in the disordered lattice. A calculation of the absolute libration frequencies of the molecules in the mixtures to the precision required here would appear practically impossible. As an indication of the sensitivity of the NQR experiment it may be noted that the change in libration frequencies required by Eq. (20) to produce a shift of 2.6 kHz in the resonance frequency is only 0.5%. However, it may be practical to develop a theory that would give reliable differences between frequencies without comparable precision in their magnitudes.

#### B. Isotope Splitting

The simplest of the solids studied is the natural abundance sample because it contains practically no  $^{15}\text{N}$ - $^{15}\text{N}$  molecules and the few  $^{14}\text{N}$ - $^{15}\text{N}$  molecules are surrounded by mostly  $^{14}\text{N}$ - $^{14}\text{N}$  molecules as neighbors. However, even this case presents a difficult theoretical problem. The  $^{14}\text{N}$ - $^{15}\text{N}$  molecule is not a member of the basis and must be treated as a defect in the lattice with two librational frequencies. These must be computed in order to obtain the averaging factor in Eq. (20). To do this requires knowing the potential, or the force constants, experienced by the defect. This problem is, of course, related to the defect volumes discussed in connection with the shift. We have not attempted to solve this problem, but it is obviously an interesting one worthy of consideration. There have been numerous general theoretical papers concerned with vibrations of isotopic mass defects in otherwise perfect lattices. In nitrogen we have an almost unique case where experimental data are available and where a meaningful com-

TABLE VI. The isotope splitting  $\nu_Q(14-15) - \nu_Q(14-14)$  at 4.2 K. Theoretical values are calculated as the difference in resonance frequencies for a pure solid of  $^{14}\text{N}-^{15}\text{N}$  molecules and a pure solid of  $^{14}\text{N}-^{14}\text{N}$  molecules, considering molecular librations only and assuming that the molecules experience identical force constants. Three theoretical values are based on published Raman frequencies for  $^{14}\text{N}-^{14}\text{N}$  molecules as referenced. Experimental value is the difference between  $\nu_Q(14-15)$  in a 46.8%  $^{15}\text{N}$  sample and  $\nu_Q(14-14)$  in a natural abundance sample.

Theory	Experiment
$10.56 \pm 0.3^a$ (kHz)	
$9.92 \pm 0.3^b$	$8.7 \pm 0.2$ (kHz)
$8.58 \pm 0.3^c$	

<sup>a</sup>Reference 5.

<sup>b</sup>Reference 6.

<sup>c</sup>Reference 7.

parison might be made with a specific theory.

The simplest procedure, theoretically, is to compare two perfect solids, one pure  $^{14}\text{N}-^{14}\text{N}$  and the other pure  $^{14}\text{N}-^{15}\text{N}$ . We shall do so assuming that the force constants are the same. The known solutions for the pure  $^{14}\text{N}-^{14}\text{N}$  lattice are then simply mass adjusted, i. e., the moment of inertia is changed and the libration frequencies for the two lattices are related by

$$\nu_i^2(14-14)/\nu_i^2(14-15) = I(14-15)/I(14-14) = \frac{30}{29}. \quad (28)$$

The contribution of the stretching vibration to  $\nu'_0$  will be different for the two kinds of molecules. The quadrupole coupling constants have not been measured for the free nitrogen molecules, but on the basis of experimental data on other isotopic molecules<sup>54,55</sup> and the predictions of two rather crude theoretical models<sup>43,55</sup> we expect  $\nu'_0(14-14)$

$> \nu'_0(14-15)$  in opposition to the solid-state isotope effect from the librations. Furthermore, the contribution of the stretching mode averaging to the isotope splitting is estimated to be not greater than a few hundred Hz, which is small enough to be neglected here. The isotope splitting is then, to a good approximation, given by

$$\Delta\nu_Q = \nu'_0 [f_i(14-15) - f_i(14-14)], \quad (29)$$

where the two averaging factors are obtained from Eqs. (28), (19), and (16). Strictly speaking, this model applies to the ordered  $^{14}\text{N}-^{15}\text{N}$  lattice. In the disordered lattice that occurs naturally the libration frequencies would be spread into a narrow band. However, because the changes are small it is very likely that physical consequences of this distinction may be ignored.

We may safely assume that the natural abundance sample is sufficiently pure that the data obtained for the  $^{14}\text{N}-^{14}\text{N}$  molecule are indistinguishable from an ideal sample; but we have no data on a pure  $^{14}\text{N}-^{15}\text{N}$  sample and therefore cannot make an exact comparison between experiment and this theoretical model. However, it is reasonable to assume that the resonance frequency  $\nu_Q(14-15)$  in a pure sample is in first order the same as the resonance frequency in a 50-50 isotopically randomly mixed sample. In the mixed sample exact translational symmetry is lost and also the libration frequencies will be spread over a certain range determined by the statistical probability of all neighboring environments in the lattice. Correspondingly, the NQR line is broadened (as observed in Fig. 7). However, the center of gravity of the resonance line should be approximately the same in the two samples because the shifts are small (first order) and the average mass

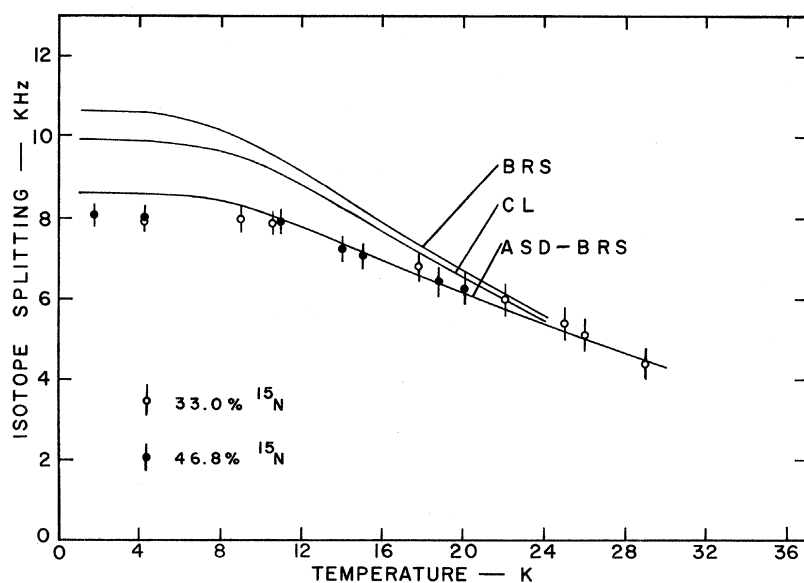


FIG. 8. Temperature dependence of the isotope splitting  $\nu_Q(14-15) - \nu_Q(14-14)$ . Experimental points with error bars are shown for two isotopic mixtures having 33.0 and 46.8%  $^{15}\text{N}$ . The three curves are theoretical calculations of the difference between the resonance frequency  $\nu_Q(14-15)$  in a solid consisting only of  $^{14}\text{N}-^{15}\text{N}$  molecules and  $\nu_Q(14-14)$  in a solid consisting only of  $^{14}\text{N}-^{14}\text{N}$  molecules, assuming identical force constants and including only the contribution of molecular librations to the motional averaging. The separate curves were calculated using published sets of Raman frequencies: BRS (Ref. 5), CL (Ref. 6), and ASD (Ref. 7).

of the system is the same. Thus, we may meaningfully compare the mass-shifted theoretical model with the experimental difference between  $\nu_Q(14-15)$  in the 46.8%  $^{15}\text{N}$  sample and  $\nu_Q(14-14)$  in the natural abundance sample. This comparison is made at 4.2 K in Table VI for the three sets of librational frequencies. Agreement is excellent for the ASD assignment, whereas the CL and BRS frequencies predict a substantially larger splitting. We believe that this is evidence for the correctness of the ASD assignment, although because of approximations in the theory it cannot be regarded as conclusive.

Absolute measurements of resonance frequencies and temperatures above 4.2 K are not sufficiently precise to deduce the difference between  $\nu_Q(14-15)$  in the 46.8%  $^{15}\text{N}$  sample and  $\nu_Q(14-14)$  in the natural abundance sample with quite the accuracy that is possible at 4.2 K. It is easier experimentally to measure the temperature dependence of the isotope splitting in a given sample. This has been done for the 33 and 46.8% concentrations. These data are shown in Fig. 8. Within experimental error there is no difference between the two mixtures. Signal strength was not adequate to follow the temperature dependence of the low abundance molecule in the other concentrations.

The theoretical temperature dependence of the splitting between two pure solids as calculated from

Eq. (30) is also shown in Fig. 8 for each set of libration frequencies. The theoretical curves match the general shape of the experimental curve very well. At high temperatures all the curves merge; furthermore the splitting approaches zero asymptotically. Thus, whereas the splitting is quite sensitive to the libration frequency assignment in the ground state, it is not at high temperatures. Mathematically, the merging of the theoretical curves at high temperature is due to the increasing dominance of a frequency independent term that appears in Eq. (30) after expansion of the functions  $\coth(\hbar\nu_Q/2kt)$ . The theoretical curve using the ASD frequencies with the BRS temperature dependence (from the observation just made the exact temperature dependence of  $\nu_l$  is not critical here) is in close agreement with the experimental splitting in Fig. 8. We may surmise that the ASD frequencies would reproduce within experimental error the entire temperature dependence of the isotope splitting as defined in Table VI.

#### ACKNOWLEDGMENTS

We gratefully acknowledge major contributions by Paul C. Canepa to the early experimental aspects of this research. His assistance has been invaluable. We have also benefitted from conversations with Professor E. R. Andrew.

- \*Research supported by a NSF Grant No. P15324.
- <sup>1</sup>T. H. Jordan, H. W. Smith, W. E. Streib, and W. N. Lipscomb, *J. Chem. Phys.* **41**, 756 (1964).
  - <sup>2</sup>W. E. Streib, T. H. Jordan, and W. N. Lipscomb, *J. Chem. Phys.* **37**, 2962 (1962).
  - <sup>3</sup>A. F. Schuch and R. L. Mills, *J. Chem. Phys.* **52**, 6000 (1970).
  - <sup>4</sup>C. A. Swenson, *J. Chem. Phys.* **23**, 1963 (1955).
  - <sup>5</sup>M. Brith, A. Ron, and O. Schnepf, *J. Chem. Phys.* **51**, 1318 (1969).
  - <sup>6</sup>J. E. Cahill and G. E. Leroy, *J. Chem. Phys.* **51**, 1324 (1969).
  - <sup>7</sup>A. Anderson, T. S. Sun, and M. C. A. Donkersloot, *Can. J. Phys.* **48**, 2265 (1970).
  - <sup>8</sup>A. Ron and O. Schnepf, *J. Chem. Phys.* **46**, 3991 (1967).
  - <sup>9</sup>R. V. St. Louis and O. Schnepf, *J. Chem. Phys.* **50**, 5177 (1969).
  - <sup>10</sup>J. A. Venables, *Phil. Mag.* **21**, 147 (1970).
  - <sup>11</sup>J. R. Brookeman and T. A. Scott (unpublished).
  - <sup>12</sup>B. C. Kohin, *J. Chem. Phys.* **33**, 882 (1960).
  - <sup>13</sup>T.-S. Kuan, A. Warshel, and O. Schnepf, *J. Chem. Phys.* **52**, 3012 (1970).
  - <sup>14</sup>O. Schnepf and A. Ron, *Discussions Faraday Soc.* **48**, 26 (1969).
  - <sup>15</sup>M. C. A. Donkersloot and S. H. Walmsley, *Mol. Phys.* **19**, 183 (1970).
  - <sup>16</sup>J. Felsteiner, D. B. Litvin, and J. Zak, *Phys. Rev. B* **3**, 2706 (1971).
  - <sup>17</sup>D. C. Heberlein, E. D. Adams, and T. A. Scott, *J. Low Temp. Phys.* **2**, 449 (1970).
  - <sup>18</sup>W. F. Giauque and I. O. Clayton, *J. Am. Chem. Soc.* **55**, 4875 (1933).
  - <sup>19</sup>M. I. Bagatskii, V. A. Kucheryany, M. G. Manzhelii, and V. A. Popov, *Phys. Status Solidi* **26**, 453 (1968).
  - <sup>20</sup>C. S. Barrett and L. Meyer, *J. Chem. Phys.* **42**, 107 (1965).
  - <sup>21</sup>T. A. Scott, *J. Chem. Phys.* **36**, 1459 (1962).
  - <sup>22</sup>P. J. Haigh and T. A. Scott, *J. Chem. Phys.* **38**, 117 (1963).
  - <sup>23</sup>A. S. DeReggi, P. C. Canepa, and T. A. Scott, *J. Mag. Res.* **1**, 144 (1969).
  - <sup>24</sup>J. R. Brookeman, P. C. Canepa, M. M. McEnnan, and T. A. Scott, *Phys. Letters* **31A**, 404 (1970).
  - <sup>25</sup>J. R. Brookeman, P. C. Canepa, and T. A. Scott, *Bull. Am. Phys. Soc.* **15**, 257 (1970).
  - <sup>26</sup>M. M. McEnnan and T. A. Scott, *Bull. Am. Phys. Soc.* **15**, 257 (1970).
  - <sup>27</sup>J. R. Brookeman, M. M. McEnnan, and T. A. Scott, *Bull. Am. Phys. Soc.* **15**, 1323 (1970).
  - <sup>28</sup>S. H. Walmsley and J. A. Pople, *Mol. Phys.* **8**, 345 (1964).
  - <sup>29</sup>M. S. Anderson and C. A. Swenson (private communication).
  - <sup>30</sup>J. L. Carolan and T. A. Scott, *J. Mag. Res.* **2**, 243 (1970).
  - <sup>31</sup>G. B. Benedek, *Magnetic Resonance at High Pressure* (Interscience, New York, 1963).
  - <sup>32</sup>F. N. H. Robinson, *J. Sci. Instr.* **36**, 481 (1959).
  - <sup>33</sup>V. G. Manzhelii, A. M. Tolkachev, and E. I. Voitovich, *Phys. Status Solidi* **13**, 351 (1966).
  - <sup>34</sup>J. H. Van Vleck, *Phys. Rev.* **74**, 1168 (1948).
  - <sup>35</sup>A. Abragam and K. Kambe, *Phys. Rev.* **91**, 894 (1953).
  - <sup>36</sup>M. M. McEnnan, dissertation (University of Florida, 1971) (unpublished).

- <sup>37</sup>C. T. O'Konski and Tae-Kyu Ha, *J. Chem. Phys.* **49**, 5354 (1968).
- <sup>38</sup>Values of  $r_{12}$  are given in Ref. 1 and by B. P. Stoich-eff, *Can. J. Phys.* **32**, 630 (1954). The error quoted here is our own estimate of uncertainty in the value of  $r_{12}$  in the solid.
- <sup>39</sup>C. J. Jameson and H. S. Gutowsky, *J. Chem. Phys.* **51**, 2790 (1969).
- <sup>40</sup>G. Binsch, J. B. Lambert, B. W. Roberts, and J. D. Roberts, *J. Am. Chem. Soc.* **86**, 5564 (1964).
- <sup>41</sup>As a purely academic comment we may note that a triplet and a doublet with the observed intensity ratios would also result if  $d$  were negligible while  $\mathcal{K}_J$  dominated with the condition  $J_{II}=J_I$ .
- <sup>42</sup>H. Bayer, *Z. Physik (Leipzig)* **130**, 227 (1951).
- <sup>43</sup>T. Kushida, *J. Sci. Hiroshima Univ. Ser. A* **19**, 327 (1957).
- <sup>44</sup>In order to obtain correct equations it is necessary to symmetrize the rotations about  $x$  and  $y$  axes because finite rotations do not commute. Equations published in the literature are sometimes in error due to neglect of this fact.
- <sup>45</sup>T. Kushida, G. B. Benedek, and N. Bloembergen, *Phys. Rev.* **104**, 1364 (1956).
- <sup>46</sup>H. S. Gutowsky and G. A. Williams, *Phys. Rev.* **105**, 464 (1957).
- <sup>47</sup>F. D. Murnaghan, *Am. J. Math.* **59**, 235 (1937).
- <sup>48</sup>P. M. Mathai and E. J. Allin (private communication).
- <sup>49</sup>One must be careful to recognize that averages of the nuclear separation  $r_{12}$  over the intramolecular stretching mode are involved that are different in the two cases. The moment of inertia is proportional to  $\langle r_{12}^2 \rangle$ , whereas the dipolar interaction goes as  $\langle r_{12}^{-3} \rangle$ . The error quoted on the value of  $r_{12}$  used encompasses these differences.
- <sup>50</sup>J. R. Brookeman, P. C. Canepa, R. Jessup, and T. A. Scott (unpublished).
- <sup>51</sup>V. S. Kogan and T. G. Omarov, *Zh. Eksperim. i Teor. Fiz.* **44**, 1873 (1963) [*Sov. Phys. JETP* **17**, 1260 (1963)].
- <sup>52</sup>P. G. Klemens, R. DeBruyn Ouboter, and C. le Pair, *Physica* **30**, 1863 (1964).
- <sup>53</sup>W. J. Mullin, *Phys. Rev. Letters* **20**, 254 (1968).
- <sup>54</sup>J. Duchesne, A. Monfils, and J. Garsou, *Physica* **22**, 816 (1956).
- <sup>55</sup>T. Tokuhiko, *J. Chem. Phys.* **47**, 109 (1967).

## Theory of the One-Phonon Resonance Raman Effect

Richard M. Martin\*

*Bell Telephone Laboratories, Murray Hill, New Jersey 07974*

(Received 19 March 1971)

Resonant enhancements of Raman scattering cross sections for photons near electronic resonances are calculated for ordinary allowed scattering and for intraband Fröhlich scattering, which is of higher order in the wave vectors and thus forbidden. Exciton effects are included exactly in the hydrogenic approximation via numerical calculations using the Green's-function formulation. Much greater enhancements are found for forbidden than for allowed lines, and it is shown that forbidden lines can become comparable to allowed lines near resonance with large Wannier excitons. It is predicted to be feasible to observe one-LO-phonon lines in crystals (e.g., TlCl and TlBr) in which such transitions are always forbidden. Comparison with experiment for CdS is presented.

### I. INTRODUCTION

Large enhancements of Raman scattering cross sections for incident or scattered photons near resonance with fundamental electronic transitions have been observed<sup>1-4</sup> and described theoretically<sup>4-11</sup> in a number of works. The present paper casts in a different form many of the calculations in previous theoretical papers and, in addition, incorporates the electron-phonon intraband Fröhlich interaction.<sup>12</sup> This part of the electron-phonon interaction has been considered previously only by Hamilton<sup>11</sup> for incident light above the band gap. In this paper it is shown to give rise to striking effects in Raman scattering just below the band gap.

All light-scattering processes in which electrons play an important role as intermediate states are expected to exhibit resonance phenomena, with

cross sections varying rapidly near allowed electronic resonances, i.e., near peaks in the absorption. Here we are interested in the frequency range just below the lowest absorption edge; the small absorption that is present in real crystals in this range plays no fundamental role and is merely a correction that must be made to experimental data.

Both electron-photon and electron-phonon interactions are here treated in perturbation theory neglecting polariton<sup>8-10,13</sup> and bound-exciton-phonon<sup>14</sup> effects. Thus the present calculations are invalid for photons sufficiently near resonance or for very large exciton-phonon interactions. Expressions for the cross section correctly coupling the exciton and photon into polaritons have been given<sup>8,9</sup> neglecting exciton dispersion, in which case they differ appreciably<sup>9,10</sup> from the perturbation expressions only for  $E_{\text{ex}} - \omega \leq E_{1t}$ , where  $E_{1t}$  is the longitudinal-trans-